

Recent Theoretical Results on
 $|\Delta I| = 3/2$ Decays of Hyperons

Jusak Tandean
Iowa State University

A. Abd El-Hady, J.T., G. Valencia
Nucl. Phys. A 651 (1999) 71

Hyperon 99
Fermilab
27 September 1999

Outline of talk

- Introduction
- Chiral Lagrangian for strong and weak interactions
- $|\Delta I| = 3/2$ decays of hyperons
 - Amplitudes to $\mathcal{O}(m_s \ln m_s)$
 - Current experimental values
 - Numerical results and discussion
- Conclusions

Introduction

Hyperon non-leptonic weak decays

$$\Sigma^+ \rightarrow n\pi^+, \quad \Sigma^+ \rightarrow p\pi^0, \quad \Sigma^- \rightarrow n\pi^-,$$

$$\Lambda \rightarrow p\pi^-, \quad \Lambda \rightarrow n\pi^0,$$

$$\Xi^- \rightarrow \Lambda\pi^-, \quad \Xi^0 \rightarrow \Lambda\pi^0.$$

- each have an S-wave, parity-violating and a P-wave, parity-conserving amplitudes
- each contains a dominant $|\Delta I| = 1/2$ and a suppressed $|\Delta I| = 3/2$ components.

The $|\Delta I| = 1/2$ transitions have been much studied in chiral perturbation theory (χ PT), and calculations including the leading non-analytic corrections have yielded mixed results.

One can get a good fit to the S-wave or P-wave amplitudes, but not both.

The $|\Delta I| = 3/2$ amplitudes are less well studied.

In view of the situation in the $|\Delta I| = 1/2$ sector, it is instructive to do a one-loop analysis of the $|\Delta I| = 3/2$ amplitudes.

Bijnens, Smeets, W. S.
Jenkins
Springer
Garofalo, Georgi
Abdel-Hady, J.T.

Chiral Lagrangian for strong and weak interactions

Octet pseudoscalar-mesons:

$$\Sigma = e^{i\phi/f}, \quad \text{where } \phi = \sqrt{2} \begin{pmatrix} \frac{1}{\sqrt{2}} \pi^0 + \frac{1}{\sqrt{6}} \eta_8 & \pi^+ & K^+ \\ \pi^- & \frac{-1}{\sqrt{2}} \pi^0 + \frac{1}{\sqrt{6}} \eta_8 & K^0 \\ K^- & \bar{K}^0 & \frac{-2}{\sqrt{6}} \eta_8 \end{pmatrix},$$

and f is the pion-decay constant in the chiral-symmetry limit.

Octet baryons:

$$B = \begin{pmatrix} \frac{1}{\sqrt{2}} \Sigma^0 + \frac{1}{\sqrt{6}} \Lambda & \Sigma^+ & p \\ \Sigma^- & \frac{-1}{\sqrt{2}} \Sigma^0 + \frac{1}{\sqrt{6}} \Lambda & n \\ \Xi^- & \Xi^0 & \frac{-2}{\sqrt{6}} \Lambda \end{pmatrix}.$$

Decuplet baryons are described by a Rarita-Schwinger field T_{abc}^μ that satisfies the constraint $\gamma_\mu T_{abc}^\mu = 0$ and is completely symmetric in its $SU(3)$ indices, a, b, c :

$$\begin{aligned} T_{111} &= \Delta^{++}, & T_{112} &= \frac{1}{\sqrt{3}} \Delta^+, & T_{122} &= \frac{1}{\sqrt{3}} \Delta^0, & T_{222} &= \Delta^-, \\ T_{113} &= \frac{1}{\sqrt{3}} \Sigma^{*+}, & T_{123} &= \frac{1}{\sqrt{6}} \Sigma^{*0}, & T_{223} &= \frac{1}{\sqrt{3}} \Sigma^{*-}, \\ T_{133} &= \frac{1}{\sqrt{3}} \Xi^{*0}, & T_{233} &= \frac{1}{\sqrt{3}} \Xi^{*-}, & T_{333} &= \Omega^-. \end{aligned}$$

Under $SU(3)_L \times SU(3)_R$ transformations,

$$\Sigma \rightarrow L \Sigma R^\dagger, \quad B \rightarrow U B U^\dagger, \quad T_{abc}^\mu \rightarrow U_{ad} U_{be} U_{cf} T_{def}^\mu,$$

where $L, R \in SU(3)_{L,R}$ and the matrix U is implicitly defined by the transformation

$$\xi \equiv e^{i\phi/(2f)} \rightarrow L \xi U^\dagger = U \xi R^\dagger.$$

In the heavy-baryon formalism (Jenkins and Manohar), the effective Lagrangian is written in terms of velocity-dependent baryon fields,

$$B_v(x) = e^{im_B \not{v} \cdot x} B(x), \quad T_v^\mu(x) = e^{im_B \not{v} \cdot x} T^\mu(x).$$

Leading-order (in energy expansion) chiral lagrangian for strong interactions:

$$\begin{aligned} \mathcal{L}^s = & \text{Tr}(\bar{B}_v i v^\mu \mathcal{D}_\mu B_v) + 2D \text{Tr}(\bar{B}_v S_v^\mu \{A_\mu, B_v\}) + 2F \text{Tr}(\bar{B}_v S_v^\mu [A_\mu, B_v]) \\ & - \bar{T}_v^\mu i v^\nu \mathcal{D}_\nu T_{v\mu} + \Delta m \bar{T}_v^\mu T_{v\mu} + C (\bar{T}_v^\mu A_\mu B_v + \bar{B}_v A_\mu T_v^\mu) + 2\mathcal{H} \bar{T}_v^\mu S_v \cdot A T_{v\mu} \\ & + \frac{1}{4} f^2 \text{Tr}(\partial^\mu \Sigma^\dagger \partial_\mu \Sigma), \end{aligned}$$

where

$$v_\mu = \frac{1}{2}(\xi \partial_\mu \xi^\dagger + \xi^\dagger \partial_\mu \xi), \quad A_\mu = \frac{i}{2}(\xi \partial_\mu \xi^\dagger - \xi^\dagger \partial_\mu \xi), \quad \mathcal{D}^\mu B_v = \partial^\mu B_v + [v^\mu, B_v],$$

$$\mathcal{D}^\mu (T_v^\nu)_{abc} = \partial^\mu (T_v^\nu)_{abc} + i \mathcal{V}_{ad}^\mu (T_v^\nu)_{dbc} + i \mathcal{V}_{bd}^\mu (T_v^\nu)_{adc} + i \mathcal{V}_{cd}^\mu (T_v^\nu)_{abd},$$

$$\bar{T}_v^\mu A_\mu B_v + \bar{B}_v A_\mu T_v^\mu = \epsilon_{abc} (\bar{T}_v^\mu)_{cde} (A_\mu)_{eb} (B_v)_{da} + \epsilon_{abc} (\bar{B}_v)_{ad} (A_\mu)_{be} (T_v^\mu)_{cde},$$

$\Delta m = m_T - m_B$, and $S_v^\mu = -\frac{1}{4} \gamma_5 [\gamma^\mu, \gamma^\nu] v_\nu$ is the velocity-dependent spin operator satisfying

$$S_v^\mu v_\mu = 0, \quad \{S_v^\mu, S_v^\nu\} = \frac{1}{2}(v^\mu v^\nu - g^{\mu\nu}), \quad [S_v^\mu, S_v^\nu] = i \epsilon^{\mu\nu\alpha\beta} v_\alpha S_{v\beta}.$$

Simplifications:

$$\text{e.g., baryon propagators: } \frac{i}{k \cdot v + i\epsilon}, \quad \frac{i}{k \cdot v + i\epsilon} (v_\mu v_\nu - g_{\mu\nu} - \frac{4}{3} S_\mu S_\nu).$$

Explicit breaking of chiral symmetry, to order m_s and in the limit $m_u = m_d = 0$, is introduced via

$$\begin{aligned} \mathcal{L}_{m_q}^s = & a \text{Tr}(M \Sigma^\dagger + \Sigma M^\dagger) \\ & + b_D \text{Tr}(\bar{B}_v \{\xi^\dagger M \xi^\dagger + \xi M^\dagger \xi, B_v\}) + b_F \text{Tr}(\bar{B}_v [\xi^\dagger M \xi^\dagger + \xi M^\dagger \xi, B_v]) \\ & + \sigma \text{Tr}(M \Sigma^\dagger + \Sigma M^\dagger) \text{Tr}(\bar{B}_v B_v) \\ & + c \bar{T}_v^\mu (\xi^\dagger M \xi^\dagger + \xi M^\dagger \xi) T_{v\mu} - \bar{\sigma} \text{Tr}(M \Sigma^\dagger + \Sigma M^\dagger) \bar{T}_v^\mu T_{v\mu}, \end{aligned}$$

where $M = \text{diag}(0, 0, m_s)$. In this limit, $m_\pi = 0$ and $m_{\eta_8}^2 = \frac{4}{3} m_K^2$, and mass splittings within the baryon octet and decuplet occur to linear order in m_s .

Within the standard model, weak transitions with $|\Delta S| = 1$ are induced by an effective Hamiltonian

$$\mathcal{H}_{\text{eff}} \sim \bar{u}_L \gamma^\mu s_L \bar{d}_L \gamma^\mu u_L + \text{h.c.},$$

that transforms as linear combination of $(8_L, 1_R)$ and $(27_L, 1_R)$.

Weak transitions with $|\Delta S| = 1$, $|\Delta I| = 3/2$ are induced by an effective Hamiltonian that transforms as $(27_L, 1_R)$ under chiral rotations:

$$\mathcal{H}_{\text{eff}}^{(27_L, 1_R)} = \frac{G_F}{\sqrt{2}} V_{ud}^* V_{us} \left(\frac{c_1 + c_2}{3} \right) 4T_{ij,kl} \bar{q}_L^i \gamma_\mu q_L^k \bar{q}_L^j \gamma^\mu q_L^l + \text{h.c.},$$

where $T_{12,13} = T_{21,13} = T_{12,31} = T_{21,31} = 1/2$ and $T_{22,23} = T_{22,32} = -1/2$.

The desired effective Lagrangian must have the symmetry structure of $\mathcal{H}_{\text{eff}}^{(27_L, 1_R)}$.

The leading-order weak Lagrangian involving baryons can be constructed from the octets \bar{B} , B and the decuplets \bar{T}_{abc} , T_{abc} using the direct products

$$8 \otimes 8 = 1 \oplus 8 \oplus 8' \oplus 10 \oplus \bar{10} \oplus 27, \quad \bar{10} \otimes 10 = 1 \oplus 8 \oplus 27 \oplus 64.$$

(Nonzero combinations involving one octet and one decuplet are of higher order.)

The leading-order weak chiral Lagrangian for baryons is, thus,

$$\mathcal{L}^w = \beta_{27} T_{ij,kl} (\xi \bar{B}_v \xi^\dagger)_{ki} (\xi B_v \xi^\dagger)_{lj} + \delta_{27} T_{ij,kl} \xi_{ka} \xi_{bi}^\dagger \xi_{lc} \xi_{cj}^\dagger (\bar{T}_v^\mu)_{abc} (T_{v\mu})_{ade} + \text{h.c.}.$$

(He & Valencia)

For purely-mesonic processes

$$\mathcal{L}_\phi^w = f \gamma_{27} T_{ij,kl} (\partial^\mu \Sigma \Sigma^\dagger)_{ki} (\partial_\mu \Sigma \Sigma^\dagger)_{lj} + \text{h.c.}$$

where γ_{27} is already fixed from $K \rightarrow \pi\pi$ decays to be $\gamma_{27} \approx 2.5 \times 10^{-9}$.

$|\Delta I| = 3/2$ decays of octet hyperons

Amplitudes to $\mathcal{O}(m_s \ln m_s)$

The amplitude for $B \rightarrow B' \pi$ in the heavy-baryon formalism

$$i\mathcal{M}_{B \rightarrow B' \pi} = G_F m_\pi^2 \bar{u}_{B'} \left(\mathcal{A}_{BB' \pi}^{(S)} + 2k \cdot S_v \mathcal{A}_{BB' \pi}^{(P)} \right) u_B,$$

where k is the outgoing four-momentum of the pion.

The $|\Delta I| = 3/2$ amplitudes satisfy the isospin relations

$$\mathcal{M}_{\Sigma^+ \rightarrow n \pi^+} - \sqrt{2} \mathcal{M}_{\Sigma^+ \rightarrow p \pi^0} + 2 \mathcal{M}_{\Sigma^- \rightarrow n \pi^-} = 0,$$

$$\mathcal{M}_{\Lambda \rightarrow n \pi^0} - \sqrt{2} \mathcal{M}_{\Lambda \rightarrow p \pi^-} = 0,$$

$$\mathcal{M}_{\Xi^0 \rightarrow \Lambda \pi^0} - \sqrt{2} \mathcal{M}_{\Xi^- \rightarrow \Lambda \pi^-} = 0,$$

and, therefore, only four of them are independent.

At one loop

$$\mathcal{A}_{BB' \pi}^{(S)} = \frac{1}{\sqrt{2} f_\pi} \left[\alpha_{BB'}^{(S)} + \left(\bar{\beta}_{BB'}^{(S)} - \bar{\lambda}_{BB' \pi} \alpha_{BB'}^{(S)} \right) \frac{m_K^2}{16\pi^2 f_\pi^2} \ln \frac{m_K^2}{\mu^2} \right],$$

$$\mathcal{A}_{BB' \pi}^{(P)} = \frac{1}{\sqrt{2} f_\pi} \left[\alpha_{BB'}^{(P)} + \left(\bar{\beta}_{BB'}^{(P)} - \bar{\lambda}_{BB' \pi} \alpha_{BB'}^{(P)} \right) \frac{m_K^2}{16\pi^2 f_\pi^2} \ln \frac{m_K^2}{\mu^2} + \gamma_{BB'} \alpha_{BB'}^{(P)} \right],$$

where $f_\pi \approx 92.4 \text{ MeV}$ is the physical pion-decay constant;

$\alpha_{BB'}$ comes from tree-level diagrams;

$\bar{\beta}_{BB'} = \beta_{BB'} + \beta'_{BB'}$ from one-loop (octet only+decuplet) decay diagrams;

$\lambda_{BB' \pi}$ from wave-function and decay-constant renormalization;

and $\gamma_{BB'}$ from the one-loop corrections to the propagator in the P-wave diagrams.

Only nonanalytic terms up to the leading logarithms ($m_s \log m_s$) are kept, the divergences being absorbed by counterterms.

The number of free parameters from counterterms is larger than that of data, and so it is possible to fit all the amplitudes to data, but there is no predictive power.

* We limit the study to evaluating the question of whether the lowest-order predictions are subject to large higher-order corrections.

(Complete one-loop calculation w/o decuplet done by Borasoy & Holstein for $\Delta I = 1/2$.)

Examples of $\mathcal{O}(p)$ weak counterterms are

$$\begin{aligned}
\mathcal{L}_1^w = & \frac{C_1}{\Lambda} T_{ij,kl} [(\xi \bar{B}_v B_v \xi^\dagger)_{ki} - (\bar{B}_v \xi^\dagger)_{ni} (\xi B_v)_{kn}] (\xi \mathcal{A} \cdot v \xi^\dagger)_{lj} \\
& + \frac{C_2}{\Lambda} T_{ij,kl} (\xi \bar{B}_v \xi^\dagger)_{ki} (\xi \{\mathcal{A} \cdot v, B_v\} \xi^\dagger)_{lj} \\
& + \frac{C_3}{\Lambda} T_{ij,kl} (\xi \bar{B}_v \xi^\dagger)_{ki} (\xi [\mathcal{A} \cdot v, B_v] \xi^\dagger)_{lj} \\
& + \frac{C_4}{\Lambda} T_{ij,kl} (\xi \{\mathcal{A} \cdot v, \bar{B}_v\} \xi^\dagger)_{ki} (\xi B_v \xi^\dagger)_{lj} \\
& + \frac{C_5}{\Lambda} T_{ij,kl} (\xi [\mathcal{A} \cdot v, \bar{B}_v] \xi^\dagger)_{ki} (\xi B_v \xi^\dagger)_{lj} \\
& + \frac{C_6}{\Lambda} T_{ij,kl} (\xi \bar{B}_v B_v \xi^\dagger)_{ki} (\xi \mathcal{A} \cdot S_v \xi^\dagger)_{lj} \\
& + \frac{C_7}{\Lambda} T_{ij,kl} (\xi \bar{B}_v \xi^\dagger)_{ki} (\xi S_v^\mu \{\mathcal{A}_\mu, B_v\} \xi^\dagger)_{lj} \\
& + \frac{C_8}{\Lambda} T_{ij,kl} (\xi \bar{B}_v \xi^\dagger)_{ki} (\xi S_v^\mu [\mathcal{A}_\mu, B_v] \xi^\dagger)_{lj} \\
& + \frac{C_9}{\Lambda} T_{ij,kl} (\xi \{\mathcal{A}_\mu, \bar{B}_v\} S_v^\mu \xi^\dagger)_{ki} (\xi B_v \xi^\dagger)_{lj} \\
& + \frac{C_{10}}{\Lambda} T_{ij,kl} (\xi [\mathcal{A}_\mu, \bar{B}_v] S_v^\mu \xi^\dagger)_{ki} (\xi B_v \xi^\dagger)_{lj} \\
& + \text{h.c.} .
\end{aligned}$$

At leading order in χ PT, $\mathcal{O}(1)$, there are contributions to the amplitudes from the tree-level Lagrangian in Eq. (3). They arise from the diagrams displayed in Figure 1 and are given by

$$\alpha_{\Sigma^+ n}^{(S)} = -\frac{3}{2}\beta_{27}, \quad \alpha_{\Sigma^- n}^{(S)} = \beta_{27}, \quad \alpha_{\Lambda p}^{(S)} = 0, \quad \alpha_{\Xi^- \Lambda}^{(S)} = 0,$$

$$\alpha_{\Sigma^+ n}^{(P)} = \left(-\frac{1}{2}D - \frac{3}{2}F\right) \frac{\beta_{27}}{m_\Sigma - m_N}, \quad \alpha_{\Sigma^- n}^{(P)} = F \frac{\beta_{27}}{m_\Sigma - m_N},$$

$$\alpha_{\Lambda p}^{(P)} = \frac{1}{\sqrt{6}}D \frac{\beta_{27}}{m_\Sigma - m_N}, \quad \alpha_{\Xi^- \Lambda}^{(P)} = -\frac{1}{\sqrt{6}}D \frac{\beta_{27}}{m_\Xi - m_\Sigma},$$

where the strong vertices in the P-wave graphs are from \mathcal{L}^s in Eq. (1).



Figure 1: Tree-level diagrams for (a) S-wave and (b) P-wave hyperon non-leptonic decays. Solid (dashed) lines denote baryon-octet (meson-octet) fields. A solid dot (hollow square) represents a strong (weak) vertex. In all figures, the strong vertices are generated by \mathcal{L}^s in Eq. (1). Here the weak vertices come from \mathcal{L}^w in Eq. (3).

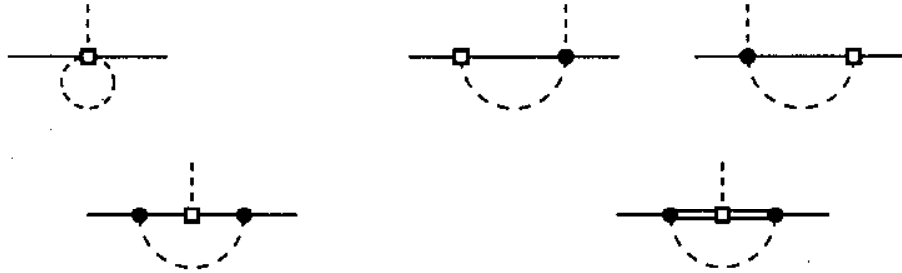


Figure 2: One-loop diagrams contributing to S-wave hyperon non-leptonic decay amplitudes, with weak vertices from \mathcal{L}^w in Eq. (3). Double (single) solid-lines represent baryon-decuplet (baryon-octet) fields.

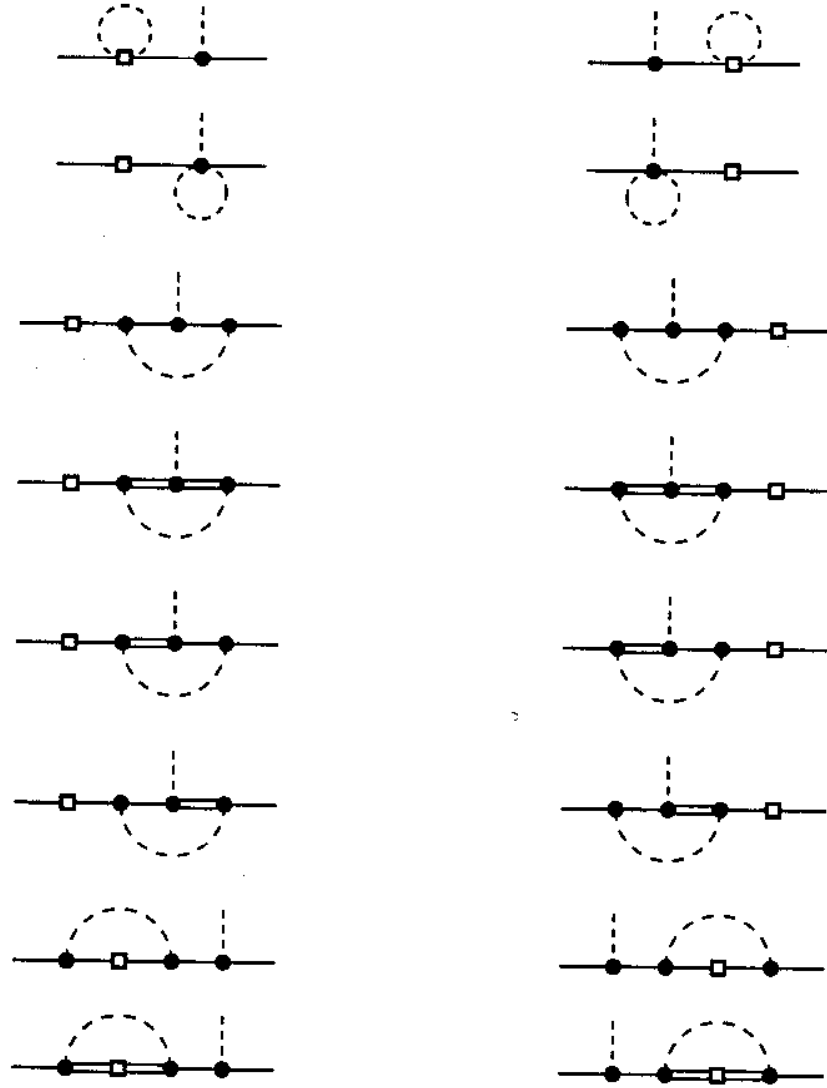


Figure 3: One-loop diagrams contributing to P-wave hyperon non-leptonic decay amplitudes, with weak vertices from \mathcal{L}^W in Eq. (3).

Contributions from one-loop diagrams involving only octet baryons, shown in Figures 2 and 3, are

$$\beta_{\Sigma^+n}^{(S)} = \left(\frac{23}{8} - \frac{5}{4}D^2 - 3DF + \frac{9}{4}F^2\right)\beta_{27}, \quad \beta_{\Lambda p}^{(S)} = 0,$$

$$\beta_{\Sigma^-n}^{(S)} = \left(-\frac{23}{12} + \frac{5}{6}D^2 + 2DF - \frac{3}{2}F^2\right)\beta_{27}, \quad \beta_{\Xi^- \Lambda}^{(S)} = 0,$$

$$\beta_{\Sigma^+n}^{(P)} = \left(\frac{29}{24}D + \frac{29}{8}F - \frac{19}{36}D^3 - \frac{29}{12}D^2F - \frac{31}{12}DF^2 + \frac{15}{4}F^3\right)\frac{\beta_{27}}{m_{\Sigma} - m_N},$$

$$\beta_{\Sigma^-n}^{(P)} = \left(-\frac{29}{12}F + \frac{8}{9}D^2F + 2DF^2 - 2F^3\right)\frac{\beta_{27}}{m_{\Sigma} - m_N},$$

$$\beta_{\Lambda p}^{(P)} = \frac{1}{\sqrt{6}}\left(-\frac{29}{12}D + \frac{16}{9}D^3 + 2D^2F - 2DF^2\right)\frac{\beta_{27}}{m_{\Sigma} - m_N},$$

$$\beta_{\Xi^- \Lambda}^{(P)} = \frac{1}{\sqrt{6}}\left(\frac{29}{12}D - \frac{16}{9}D^3 + 2D^2F + 2DF^2\right)\frac{\beta_{27}}{m_{\Xi} - m_{\Sigma}}.$$

One-loop diagrams involving decuplet baryons (also shown in Figures 2 and 3) yield

$$\beta'_{\Sigma^+n}{}^{(S)} = -\frac{1}{3}C^2\delta_{27}, \quad \beta'_{\Lambda p}{}^{(S)} = 0,$$

$$\beta'_{\Sigma^-n}{}^{(S)} = \frac{2}{9}C^2\delta_{27}, \quad \beta'_{\Xi^- \Lambda}{}^{(S)} = 0,$$

$$\beta'_{\Sigma^+n}{}^{(P)} = \left(\frac{85}{162}\mathcal{H} - \frac{35}{27}D + \frac{1}{9}F\right)C^2\frac{\beta_{27}}{m_{\Sigma} - m_N} - \left(\frac{1}{9}D + \frac{1}{3}F\right)C^2\frac{\delta_{27}}{m_{\Sigma} - m_N},$$

$$\beta'_{\Sigma^-n}{}^{(P)} = \left(-\frac{25}{54}\mathcal{H} + \frac{26}{27}D - \frac{2}{9}F\right)C^2\frac{\beta_{27}}{m_{\Sigma} - m_N} + \frac{2}{9}FC^2\frac{\delta_{27}}{m_{\Sigma} - m_N},$$

$$\beta'_{\Lambda p}{}^{(P)} = \frac{1}{\sqrt{6}}\left(-\frac{5}{54}\mathcal{H} + \frac{4}{3}D + \frac{4}{3}F\right)C^2\frac{\beta_{27}}{m_{\Sigma} - m_N} + \frac{2}{9\sqrt{6}}DC^2\frac{\delta_{27}}{m_{\Sigma} - m_N},$$

$$\beta'_{\Xi^- \Lambda}{}^{(P)} = \frac{1}{\sqrt{6}}\left(\frac{5}{54}\mathcal{H} - \frac{4}{3}D - \frac{4}{3}F\right)C^2\frac{\beta_{27}}{m_{\Xi} - m_{\Sigma}} - \frac{1}{\sqrt{6}}DC^2\frac{\delta_{27}}{m_{\Xi} - m_{\Sigma}}.$$

The contributions from the wave-function renormalization of the pion and the octet baryons and from the renormalization of the pion-decay constant are collected into

$$\bar{\lambda}_{BB'\pi} = \frac{1}{2}(\bar{\lambda}_B + \bar{\lambda}_{B'} + \lambda_\pi) - \lambda_f,$$

where $\bar{\lambda}_B = \lambda_B + \lambda'_B$, λ_π and λ_f are defined by

$$Z_B = 1 + \bar{\lambda}_B \frac{m_K^2}{16\pi^2 f_\pi^2} \ln \frac{m_K^2}{\mu^2}, \quad Z_\pi = 1 + \lambda_\pi \frac{m_K^2}{16\pi^2 f_\pi^2} \ln \frac{m_K^2}{\mu^2},$$

and

$$\frac{f_\pi}{f} = 1 + \lambda_f \frac{m_K^2}{16\pi^2 f_\pi^2} \ln \frac{m_K^2}{\mu^2},$$

with

$$\lambda_N = \frac{17}{6}D^2 - 5DF + \frac{15}{2}F^2, \quad \lambda'_N = \frac{1}{2}C^2,$$

$$\lambda_\Lambda = \frac{7}{3}D^2 + 9F^2, \quad \lambda'_\Lambda = C^2,$$

$$\lambda_\Sigma = \frac{13}{3}D^2 + 3F^2, \quad \lambda'_\Sigma = \frac{7}{3}C^2,$$

$$\lambda_\Xi = \frac{17}{6}D^2 + 5DF + \frac{15}{2}F^2, \quad \lambda'_\Xi = \frac{13}{6}C^2,$$

$$\lambda_\pi = -\frac{1}{3}, \quad \lambda_f = -\frac{1}{2}.$$

For numerical estimates, we use the values (Jenkins & Manohar)

$$D = 0.61 \pm 0.04, \quad F = 0.40 \pm 0.03, \quad C = 1.6, \quad \mathcal{H} = -1.9 \pm 0.7.$$

Finally, for the P-waves, we must also include one-loop corrections to the propagator that appears in tree-level pole diagrams:

$$\gamma_{\Sigma^+ n} = \gamma_{\Sigma^- n} = \gamma_{\Lambda p} = \frac{\mu_{\Sigma N}}{m_{\Sigma} - m_N}, \quad \gamma_{\Xi^- \Lambda} = \frac{\mu_{\Xi \Sigma}}{m_{\Xi} - m_{\Sigma}},$$

where

$$\mu_{XY} = -(\bar{\beta}_X - \bar{\beta}_Y) \frac{m_K^3}{16\pi f_\pi^2} + [(\bar{\gamma}_X - \bar{\gamma}_Y - \bar{\lambda}_X \alpha_X + \bar{\lambda}_Y \alpha_Y) m_s + (\lambda'_X - \lambda'_Y) \Delta m] \frac{m_K^2}{16\pi^2 f_\pi^2} \ln \frac{m_K^2}{\mu^2},$$



and

$$\alpha_N = -2(b_D - b_F) - 2\sigma, \quad \alpha_{\Sigma} = -2\sigma, \quad \alpha_{\Xi} = -2(b_D + b_F) - 2\sigma,$$

$$\bar{\beta}_N = \frac{5}{3}D^2 - 2DF + 3F^2 + \frac{4}{9\sqrt{3}}(D^2 - 6DF + 9F^2) + \frac{1}{3}C^2,$$

$$\bar{\beta}_{\Sigma} = 2D^2 + 2F^2 + \frac{16}{9\sqrt{3}}D^2 + \left(\frac{10}{9} + \frac{8}{9\sqrt{3}}\right)C^2,$$

$$\bar{\beta}_{\Xi} = \frac{5}{3}D^2 + 2DF + 3F^2 + \frac{4}{9\sqrt{3}}(D^2 + 6DF + 9F^2) + \left(1 + \frac{8}{9\sqrt{3}}\right)C^2,$$

$$\bar{\gamma}_N = \frac{43}{9}b_D - \frac{25}{9}b_F - b_D\left(\frac{4}{3}D^2 + 12F^2\right) + b_F\left(\frac{2}{3}D^2 - 4DF + 6F^2\right) + \frac{52}{9}\sigma - 2\sigma\lambda_N + \frac{1}{3}cC^2 - 2\tilde{\sigma}\lambda'_N,$$

$$\bar{\gamma}_{\Sigma} = 2b_D - b_D(6D^2 + 6F^2) - b_F(12DF) + \frac{52}{9}\sigma - 2\sigma\lambda_{\Sigma} + \frac{8}{9}cC^2 - 2\tilde{\sigma}\lambda'_{\Sigma},$$

$$\bar{\gamma}_{\Xi} = \frac{43}{9}b_D + \frac{25}{9}b_F - b_D\left(\frac{4}{3}D^2 + 12F^2\right) - b_F\left(\frac{2}{3}D^2 + 4DF + 6F^2\right) + \frac{52}{9}\sigma - 2\sigma\lambda_{\Xi} + \frac{29}{9}cC^2 - 2\tilde{\sigma}\lambda'_{\Xi}.$$

Parameter values:

$$b_D m_s = \frac{3}{8}(m_{\Sigma} - m_{\Lambda}) \approx 0.0290 \text{ GeV},$$

$$b_F m_s = \frac{1}{4}(m_N - m_{\Xi}) \approx -0.0948 \text{ GeV},$$

$$c m_s = \frac{1}{2}(m_{\Omega} - m_{\Delta}) \approx 0.220 \text{ GeV},$$

$$\Delta m - 2(\tilde{\sigma} - \sigma) m_s = m_{\Delta} - m_{\Sigma} \approx 0.0389 \text{ GeV},$$

where the fourth parameter is the only combination of Δm , σm_s , and $\tilde{\sigma} m_s$, which occurs in μ_{XY} .

Current experimental values

The value of the S- and P-wave amplitudes for each hyperon decay $B \rightarrow B'\pi$ can be extracted from the measurement of the decay rate Γ and asymmetry parameters α and γ ,

$$\Gamma = \frac{G_F^2 m_\pi^4}{8\pi} |\mathbf{k}| \frac{(m_B - m_{B'})^2 - m_\pi^2}{m_B^2} (|s|^2 + |p|^2) ,$$

$$\alpha = \frac{2 \operatorname{Re}(s^* p)}{|s|^2 + |p|^2} , \quad \gamma = \frac{|s|^2 - |p|^2}{|s|^2 + |p|^2} ,$$

where s and p are related to $\mathcal{A}_{BB'\pi}^{(S,P)}$ by

$$s = \mathcal{A}^{(S)} , \quad p = -|\mathbf{k}| \mathcal{A}^{(P)} ,$$

\mathbf{k} being the pion three-momentum in the rest frame of the decaying baryon.

Table 1: Experimental values for S- and P-wave amplitudes.

Decay mode	s	p
$\Sigma^+ \rightarrow n\pi^+$	0.06 ± 0.01	1.85 ± 0.01
$\Sigma^+ \rightarrow p\pi^0$	-1.48 ± 0.05	1.21 ± 0.06
$\Sigma^- \rightarrow n\pi^-$	1.95 ± 0.01	-0.07 ± 0.01
$\Lambda \rightarrow p\pi^-$	1.46 ± 0.01	0.53 ± 0.01
$\Lambda \rightarrow n\pi^0$	-1.09 ± 0.02	-0.40 ± 0.03
$\Xi^- \rightarrow \Lambda\pi^-$	-2.06 ± 0.01	0.50 ± 0.02
$\Xi^0 \rightarrow \Lambda\pi^0$	1.55 ± 0.02	-0.33 ± 0.02

From the amplitudes in Table 1, we can extract the $|\Delta I| = 3/2$ components using the relations

$$S_3^{(\Lambda)} = \frac{1}{\sqrt{3}} \left(\sqrt{2} s_{\Lambda \rightarrow n\pi^0} + s_{\Lambda \rightarrow p\pi^-} \right), \quad S_3^{(\Xi)} = \frac{2}{3} \left(\sqrt{2} s_{\Xi^0 \rightarrow \Lambda\pi^0} + s_{\Xi^- \rightarrow \Lambda\pi^-} \right),$$

$$S_3^{(\Sigma)} = -\sqrt{\frac{5}{18}} \left(s_{\Sigma^+ \rightarrow n\pi^+} - \sqrt{2} s_{\Sigma^+ \rightarrow p\pi^0} - s_{\Sigma^- \rightarrow n\pi^-} \right),$$

the $|\Delta I| = 1/2$ components (for Λ and Ξ decays)

$$S_1^{(\Lambda)} = \frac{1}{\sqrt{3}} \left(s_{\Lambda \rightarrow n\pi^0} - \sqrt{2} s_{\Lambda \rightarrow p\pi^-} \right), \quad S_1^{(\Xi)} = \frac{\sqrt{2}}{3} \left(s_{\Xi^0 \rightarrow \Lambda\pi^0} - \sqrt{2} s_{\Xi^- \rightarrow \Lambda\pi^-} \right),$$

and analogous ones for the P-waves. The $|\Delta I| = 1/2$ rule for hyperon decays can be seen in the ratios shown in Table 2.

Table 2: Experimental values of ratios of $|\Delta I| = 3/2$ to $|\Delta I| = 1/2$ amplitudes.

$S_3^{(\Lambda)}/S_1^{(\Lambda)}$	$S_3^{(\Xi)}/S_1^{(\Xi)}$	$S_3^{(\Sigma)}/s_{\Sigma^- \rightarrow n\pi^-}$
0.026 ± 0.009	0.042 ± 0.009	-0.055 ± 0.020
$P_3^{(\Lambda)}/P_1^{(\Lambda)}$	$P_3^{(\Xi)}/P_1^{(\Xi)}$	$P_3^{(\Sigma)}/p_{\Sigma^+ \rightarrow n\pi^+}$
0.031 ± 0.037	-0.045 ± 0.047	-0.059 ± 0.024

Numerical results and discussion

$$\mathcal{L}^{\nu} = \beta_{27} T_{ij,kl} (\xi \bar{B}_\nu \xi^\dagger)_{ki} (\xi B_\nu \xi^\dagger)_{lj} + \delta_{27} T_{ij,kl} \xi_{kd} \xi_{bi}^\dagger \xi_{le} \xi_{cj}^\dagger (\bar{T}_\nu^\mu)_{abc} (T_{\nu\mu})_{ade} + \text{h.c.} .$$

$$\mathcal{M}_{\text{tree}} = C_1 \beta_{27} , \quad \mathcal{M}_{\text{loop}}^{\text{octet}} = C_2 \beta_{27} , \quad \mathcal{M}_{\text{loop}}^{\text{decuplet}} = C_3 \beta_{27} + C_4 \delta_{27} .$$

Table 3: Summary of results for $|\Delta I| = 3/2$ components of the S- and P-wave amplitudes to $\mathcal{O}(m_s \ln m_s)$. We use $\beta_{27} = \delta_{27} = -0.068 \sqrt{2} f_\pi G_F m_\pi^2$ and $\mu = 1 \text{ GeV}$.

Amplitude	Experiment	Theory		
		Tree	Octet	Decuplet
		$\mathcal{O}(1)$	$\mathcal{O}(m_s \ln m_s)$	$\mathcal{O}(m_s \ln m_s)$
$S_3^{(\Lambda)}$	-0.047 ± 0.017	0	0	0
$S_3^{(\Xi)}$	0.088 ± 0.020	0	0	0
$S_3^{(\Sigma)}$	-0.107 ± 0.038	-0.107	-0.089	-0.084
$P_3^{(\Lambda)}$	-0.021 ± 0.025	0.012	0.005	-0.060
$P_3^{(\Xi)}$	0.022 ± 0.023	-0.037	-0.022	0.065
$P_3^{(\Sigma)}$	-0.110 ± 0.045	0.032	0.015	-0.171

- Calculations yield zero contributions to $S_3^{(\Lambda)}$ and $S_3^{(\Xi)}$, indicating that they are predicted to be about 1/3 of $S_3^{(\Sigma)}$ in size because there are nonvanishing contributions from operators occurring at the next order, $\mathcal{O}(m_s/\Lambda_{\chi\text{SB}})$. The experimental values of $S_3^{(\Lambda)}$ and $S_3^{(\Xi)}$ support this prediction.

- Since only nonanalytic loop terms are kept, and since errors in the measured P-wave amplitudes are larger than those in the S-wave ones, we extract β_{27} by fitting the tree-level $S_3^{(\Sigma)}$ to experiment, and treat the tree-level P-waves as predictions and the loop results as a measure of the uncertainties of the lowest-order predictions.

$$\mathcal{M}_{\text{tree}} = C_1 \beta_{27}, \quad \mathcal{M}_{\text{loop}}^{\text{octet}} = C_2 \beta_{27}, \quad \mathcal{M}_{\text{loop}}^{\text{decuplet}} = C_3 \beta_{27} + C_4 \delta_{27}.$$

Table 1: Summary of results for $|\Delta I| = 3/2$ components of the S- and P-wave amplitudes to $\mathcal{O}(m_s \ln m_s)$. We use $\beta_{27} = \delta_{27} = -0.068 \sqrt{2} f_\pi G_F m_\pi^2$ and $\mu = 1 \text{ GeV}$.

Amplitude	Experiment	Theory		
		Tree $\mathcal{O}(1)$	Octet $\mathcal{O}(m_s \ln m_s)$	Decuplet $\mathcal{O}(m_s \ln m_s)$
$S_3^{(\Sigma)}$	-0.107 ± 0.038	-0.107	-0.089	-0.084
$P_3^{(\Lambda)}$	-0.021 ± 0.025	0.012	0.005	-0.060
$P_3^{(\Xi)}$	0.022 ± 0.023	-0.037	-0.022	0.065
$P_3^{(\Sigma)}$	-0.110 ± 0.045	0.032	0.015	-0.171

- The lowest-order P-wave predictions are not impressive, but they have the right order of magnitude and differ from the central value of the measurements by at most three standard deviations.

For comparison, in the $|\Delta I| = 1/2$ case the tree-level predictions for the P-wave amplitudes differ from the measurements by factors of up to 20.

- The loop corrections depend on β_{27} and δ_{27} .

For illustrative purposes, we choose $\delta_{27} = \beta_{27}$, a choice consistent with dimensional analysis and the normalization of \mathcal{L}^w .

- Some of the loop corrections are comparable to or even larger than the lowest-order results although they are expected to be smaller by about $M_K^2/(4\pi f_\pi)^2 \approx 0.2$.

Large corrections occur when several diagrams add up constructively, resulting in deviations of up to an order of magnitude from power-counting expectations, as the expansion parameter is not sufficiently small.

These numbers are consistent with naive expectations.

- Although the one-loop corrections are large, they are all much smaller than their counterparts in $|\Delta I| = 1/2$ transitions, where they can be as large as 30 times the lowest-order amplitude in the case of the P-wave in $\Lambda^* \rightarrow p\pi^+$.

This discrepancy was due to an anomalously small lowest-order prediction arising from the cancellation of two nearly identical terms.

Table 2: Experimental and theoretical values of S- and P-wave $|\Delta I| = 1/2$ amplitudes.

Decay mode	s_{expt}	s_{theory}	s_{tree}	s_{loop}	$s_{\text{loop}}^{(\text{oct})}$	$s_{\text{loop}}^{(\text{dec})}$
$\Sigma^+ \rightarrow n\pi^+$	0.06	-0.09	0.00	-0.09	0.13	-0.22
$\Sigma^- \rightarrow n\pi^-$	1.88	1.88	1.62	0.26	0.40	-0.14
$\Lambda \rightarrow p\pi^-$	1.42	1.42	0.61	0.81	0.24	0.58
$\Xi^- \rightarrow \Lambda\pi^-$	-1.98	-1.98	-1.29	-0.69	-0.22	-0.46
Decay mode	p_{expt}	p_{theory}	p_{tree}	p_{loop}	$p_{\text{loop}}^{(\text{oct})}$	$p_{\text{loop}}^{(\text{dec})}$
$\Sigma^+ \rightarrow n\pi^+$	1.81	2.41	-0.40	2.81	0.07	2.74
$\Sigma^- \rightarrow n\pi^-$	-0.06	1.93	-0.16	2.10	0.08	2.01
$\Lambda \rightarrow p\pi^-$	<u>0.52</u>	-1.13	<u>-0.03</u>	<u>-1.10</u>	-0.09	-1.01
$\Xi^- \rightarrow \Lambda\pi^-$	<u>0.48</u>	2.17	-0.22	2.39	0.06	2.33

Conclusions

A discussion of $|\Delta I| = 3/2$ amplitudes for hyperon decays in χ PT has been presented.

- At leading order these amplitudes are described in terms of only one weak parameter, which can be fixed from the observed value of the S-wave amplitudes in Σ decays.
- After fitting this number, we have predicted the P-waves and used our one-loop calculation to discuss uncertainties of the lowest-order predictions.
- Our predictions are not contradicted by current data, but current experimental errors are too large for a meaningful conclusion.
- We have shown that the one-loop nonanalytic corrections have the relative size expected from naive power counting.

The combined experimental efforts of E871 and KTeV could give us improved accuracy in the measurements of some of the decay modes that we have discussed and allow a more quantitative comparison of theory and experiment.